

Using sensorless direct torque with fuzzy proportional-integral controller to control three phase induction motor

Yaser Nabeel Ibrahim Alothman¹, Wisam Essmat Abdul-Lateef², Sabah Abdul-Hassan Gitaffa³

¹Department of Control and Systems Engineering, University of Technology, Baghdad, Iraq

²Department of Electromechanical Engineering, University of Technology, Baghdad, Iraq

³Department of Electrical Engineering, University of Technology, Baghdad, Iraq

Article Info

Article history:

Received Apr 21, 2022

Revised Jun 28, 2022

Accepted Sep 30, 2022

Keywords:

Direct torque control
Extended kalman filter
Fuzzy PI controller
Grey wolf optimizer
Induction motor

ABSTRACT

Induction motors (IM) attracted many researchers in the last few decades. In this field, various applications are implemented, such as servo motor drives and electric vehicles. This work applies a sensorless direct torque controller (DTC) to control a three-phase IM. System dynamics of the IM were derived. A nonlinear dynamic model had introduced with white noise. Given the complexity of the dynamics, the Jacobean Linearization technique has been used to obtain the linear model for a control task. A DTC technique is employed to control the motor speed of the system with a combination of two controllers. The fuzzy proportional-integral (PI) controllers are applied to obtain the reference torque based on an optimization process against the speed error raise. The optimizer is called grey wolf optimizer (GWO) and is implemented to achieve the centre values of the two output memberships for the fuzzy PI controllers. Then the extended Kalman filter (EKF) is used to evaluate the direct and quadratic components of the rotor flux and rotor speed from the observation of stator voltages and currents. The system is tested employing MATLAB simulation software and determines the targeted results. The outcomes are evaluated to improve the control performance.

This is an open access article under the [CC BY-SA](#) license.



Corresponding Author:

Yaser Nabeel Ibrahim Alothman

Department of Control and Systems Engineering, University of Technology

52 street, Baghdad, Iraq

Email: 60005@uotechnology.edu.iq

1. INTRODUCTION

Most industrial drive applications employ induction motors (IM). Many control algorithms of IM have constituted two main categories; scalar control and vector control. Scalar control contains an open-loop voltage and or frequency control, slip hesitation with voltage control, and frequent slip with the current controller [1]. The vector controls are costly and high-rendition drives whose objective is controlling the quantity and the voltage phase or the current vectors. The control vector is categorized into two types; the field orientation control (FOC) and the direct torque control (DTC) strategies [2]. FOC provides a behaviour of the IM that is identical to that of the DC motor with a separation between the flux and torque. This decoupling supplies rapid torque action, a high-pace control ambit and summit performance for a broad load domain. Nonetheless, the controller furthermore has a heightened sensibility from the parametric contrasts for the apparatus [2]. The torque is controlled by adjustment of the quadratic ingredient of the stator current. In the direct FOC, a flux estimator is considered, on the other hand, a mechanic pace sensor is required. This approach is quite a detector of the constant rotor duration.

The basic concepts of the FOC method were chosen by Manias [3]. Research by Takahashi and Noguchi [4], a conventional proportional-integral (PI) compared to that of the PI-like fuzzy is designed to

control IM speed [5], while the FOC with that of use PI and I-P controllers had established using MATLAB simulation. The FOC approach is employed to design the I-P controller, and comparison has been taken into account to obtain a better performance. The DTC control techniques are categorized into two varieties typical and modern DTC strategies. Modern DTC is classified into adjusted switching table, neural network controller, fuzzy logic controller, genetic algorithm, model predictive controller, space vector modulation, and sliding mode controller based [6]-[9]. The amendments are executed in the essentially switching table by applying all the voltage vectors based on a suitable concatenation. These are performed by subjected to two approaches namely; six-sector and twelve-sector tables [10], [11]. The sensorless control design of an IM means that the proposed controller has been applied without any speed sensor. Speed estimation techniques are classified as: slip calculation (calculate the speed from slip frequency), direct synthesis from state equations (estimates the motor speed from rotor fluxes), luenberger observer (LO) technique, the observer namely sliding mode observer (SMO), extended Kalman filter (EKF), and optimized model reference adaptive controller (MRAC).

In model reference adaptive systems (MRAS), the response of the reference model is compared with the required outcomes of the adaptive model till the error between them becomes zero. To estimate the speed error PI-control is applied [12]. However, PI tuning parameters are hard to achieve with time consumption appears. The adaptive flux observer LO that uses for the sensorless IM model is an observer to handle it. Considerable of this device model and a feedback loop with calculated stator current and rotor flux. Nevertheless, based on Lyapunov stability, the gaining matrix of the top-order observer has to be designed. Therefore, the observer has to be faster than the monitored system. The LO is an adaptive flux observer without noise. A discrete EKF (DEKF) in [13]; is employed to estimate the system state of the synchronous motor with a two-phase permanent magnet (PMSM). The linearized model is applied, and the errors eliminated to overcome the system uncertainty and noise. The functional order PI-controller for PMSM is employed [14], considering particle swarm optimization and superior performance obtained. Research by Wang *et al.* [15], the stability of the observer is proved based on Lyapunov theory. The SMO estimates the system states in the form of precisely converging with that of the actual outcomes of the plant. Consequently, the capability to generate a sliding motion for the error between the measured and the observer outcomes is improved.

In this paper, the EKF is an optimum stochastic observer applied to estimate the state variables of nonlinear systems; recursively. The EKF noise sources considered lack of accuracy obtained from the system modelling and measurements. In the scenario of the error reduction, the estimation process of the EKF is achieved recursively to demonstrate the story of the error approaching zero. The form of the EKF may be considered a continuous, discrete, or hybrid type. The filter operation depends on the prediction process and correction process. While the noise of the system and observation noise is white Gaussian form. When the error covariance matrices are recognized EKF works properly. The system states have extended due to the linearization of nonlinearity by using Jacobian linearization [16]. This paper is structured as pursues; i) introduction, ii) DTC strategy, iii) the IM mathematical model, iv) provide an EKF, v) points to a fuzzy-PI control system designed and introduced along simulation, vi) presents a grey wolf optimizer (GWO), vii) provides simulation results and analysis, and viii) targets the conclusion with future works.

2. RESEARCH METHOD

2.1. The DTC strategy

The DTC scheme has clarified in Figure 1. To handle the designed torque for the dynamic model, the inverter states are selected such that the vector of stator flux is in the form of stopped, deaccelerated, or accelerated. The output signal of the torque hysteresis controller (δ_T) is with values of -1, 0, and 1. The output signal of the flux hysteresis controller (δ_λ) has values of 0 and 1. The d-q plane shown in Figure 2 separates into six sectors [2]. The control design of the torque is the chosen values of the inverter state that rely on the sector values of the stator vector plane. Then the direction of rotation of the motor is shown in Table 1 [2].

The control design of the flux hysteresis is in charge of displacing the stator flux over the nomination path depending on the imposes of the voltage vector for the stator (V1-V6). By consideration, hysteresis control torque obtains the period for the zero-value voltage vectors (V0, V7) that retain the torque in the known hysteresis tolerance boundary. This hysteresis band-related flux control is responsible for the limitations of the high flux value. The torque ripple is influenced by the torque hysteresis boundary's width only while staying independently of the stator part of the flux hysteresis boundary's width [17]. When the band of the torque hysteresis reduces, then the frequency of the switching rises and the losses for the inverter switching is going to increase. The stator measurement of the current and the voltage are imported from the motor stator that converted into double phase fixed frame coordinates. An intelligent controller is implemented in [18] to eliminate the outcomes' ripples of the motor system.

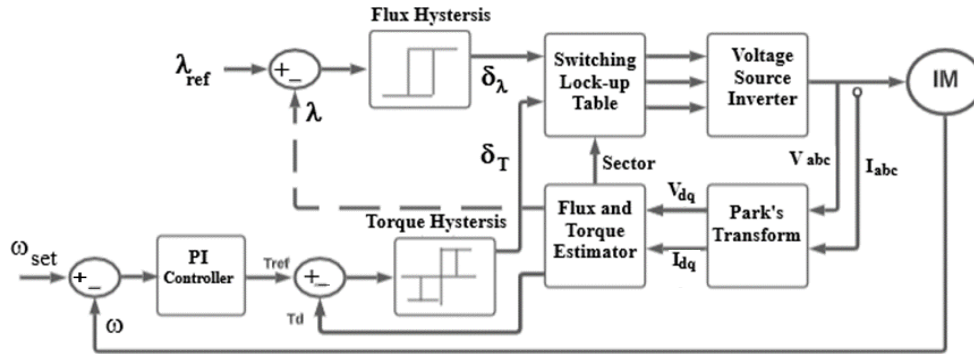


Figure 1. DTC scheme

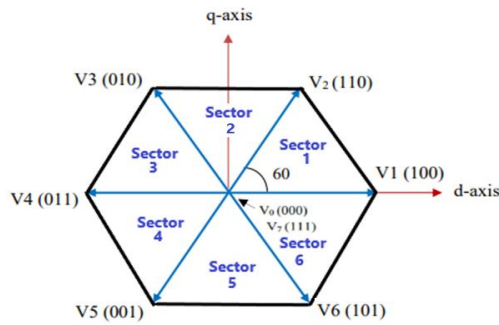


Figure 2. Stator voltage vectors

Table 1. The inverter of voltage vectors

δ_λ	δ_T	S1	S2	S3	S4	S5	S6
1	1	V2	V3	V4	V5	V6	V1
1	0	V0	V7	V0	V7	V0	V7
1	-1	V6	V1	V2	V3	V4	V5
0	1	V3	V4	V5	V6	V1	V2
0	0	V7	V0	V7	V0	V7	V0
0	-1	V5	V6	V1	V2	V3	V4

2.2. Modelling of induction motor

According to the motor equivalent circuit in the dq frame, the rate of change of rotor flux components is described by [19], [20].

$$\frac{d}{dt}(\lambda_{dr}) = -\frac{R_r}{L_r}\lambda_{dr} - \omega\lambda_{qr} - \frac{L_m R_r}{L_r}(i_{ds}) \quad (1)$$

$$\frac{d}{dt}(\lambda_{qr}) = -\frac{R_r}{L_r}\lambda_{qr} + \omega\lambda_{dr} + \frac{L_m R_r}{L_r}(i_{qs}) \quad (2)$$

Where:

λ_{qr} and λ_{dr} are the rotor flux quadratic and direct component

L_r is the inductance of the system rotor

L_m is the mutual rotor inductance

L_s and R_s are both inductance and resistance of the stator

i_{qs} and i_{ds} are the stator current quadratic and direct components

V_{qs} and V_{ds} are the stator voltage quadratic and direct components

i_{qr} and i_{dr} are the rotor current quadratic and direct components

The rate of change of stator currents components are given by [19], [20].

$$\frac{d}{dt}(i_{ds}) = -\left(\frac{L_m^2 R_r + L_r^2 R_s}{\sigma L_s L_r^2}\right)i_{ds} + \left(\frac{L_m R_r}{\sigma L_s L_r^2}\right)\lambda_{dr} + \left(\frac{L_m \omega}{\sigma L_s L_r}\right)\lambda_{qr} + \frac{1}{\sigma L_s} V_{ds} \quad (3)$$

$$\frac{d}{dt}(i_{qs}) = -\left(\frac{L_m^2 R_r + L_r^2 R_s}{\sigma L_s L_r^2}\right) i_{qs} + \left(\frac{L_m R_r}{\sigma L_s L_r^2}\right) \lambda_{qr} - \left(\frac{L_m \omega}{\sigma L_s L_r}\right) \lambda_{dr} + \frac{1}{\sigma L_s} V_{qs} \quad (4)$$

Where R_r is the resistance of the rotor; p is the poles number; and ω is the angular rotor pace.

The angular acceleration of the model rotor is equivalent to the torques summation that influences the rotor divided by the inertia of the rotor, where the speed is as (5):

$$\frac{d}{dt}(\omega) = \frac{1}{J} (T_e - T_L) \quad (5)$$

where T_L and T_e are the load and the developed torques, respectively and J is the moment of inertia for the rotor. Developed torque may be calculated by [19], [20]:

$$T_e = \left(\frac{p L_m}{3 L_r}\right) (i_{qs} \lambda_{dr} - i_{ds} \lambda_{qr}) \quad (6)$$

2.3. Extended Kalman filter

The EKF is an estimator filter employed to recognize the speed and position rotor relying on measured values such as stator currents and stator voltages. The motor model is nonlinear with random white noise (w), while the nonlinear observation is with random white noise (v). The nonlinearity in the motor system and its observation needs an extension in the filter states based on Jacobean linearization. The motor model is described by:

$$\hat{x}_{n+1} = A \hat{x}_n + B u_n + w \quad (7)$$

$$y_n = H x_n + v \quad (8)$$

where the state $x^T = [i_{ds} \ i_{qs} \ \lambda_{dr} \ \lambda_{qr} \ \omega]$ and the output $y^T = [i_{ds} \ i_{qs}]$, as well as $u_n^T = [V_{ds} \ V_{qs}]$.

The matrices of the discrete-time system is:

$$A_n = \begin{bmatrix} A_{11} & 0 & A_{13} & A_{14} & A_{15} \\ 0 & A_{22} & A_{23} & A_{24} & A_{25} \\ A_{31} & 0 & A_{33} & A_{34} & A_{35} \\ 0 & A_{42} & A_{43} & A_{44} & A_{45} \\ 0 & 0 & 0 & 0 & 1 \end{bmatrix}, B = T \begin{bmatrix} B_1 & 0 \\ 0 & B_1 \\ 0 & 0 \\ 0 & 0 \\ 0 & 0 \end{bmatrix}, H = \begin{bmatrix} 1 & 0 & 0 & 0 & 0 \\ 0 & 1 & 0 & 0 & 0 \end{bmatrix}$$

$$A_{11} = A_{22} = 1 - \frac{T}{\sigma} \left(\frac{R_s}{L_s} + \frac{1 - \sigma}{\tau_r} \right)$$

$$A_{13} = A_{24} = \frac{\varepsilon}{\tau_r} \quad A_{31} = A_{42} = L_m T / \tau_r$$

$$A_{14} = -A_{23} = \varepsilon \omega \quad A_{15} = \varepsilon \lambda_{qr}$$

$$A_{25} = -\varepsilon \lambda_{dr} \quad A_{34} = -A_{43} = -T \omega$$

$$A_{33} = A_{44} = 1 - T / \tau_r$$

$$A_{35} = -T \lambda_{qr} \quad A_{45} = T \lambda_{dr}$$

$$\tau_r = \frac{L_r}{R_r} \quad \sigma = 1 - \frac{L_m^2}{L_r L_s}$$

$$\varepsilon = \frac{L_m T}{\sigma L_s L_r} \quad B_1 = \frac{1}{\sigma L_s}$$

The EKF procedure steps are [21]:

Step 1: prediction of state

$$x'_n = \Phi \hat{x}_n \quad (9)$$

where Φ is the transfer function defined from (1) to (6)

Step 2: prediction of error covariance matrix

$$P' = A_n P A_n^T + Q \quad (10)$$

where Q is the system covariance matrix ($E(w w^T)$)

Step 3: determine the Kalman filter's gain (K)

$$K = P' H (H P' H^T + R)^{-1} \quad (11)$$

where R is the observation covariance matrix ($E(v v^T)$)

Step 4: modification of the state estimation

$$\hat{x}_{n+1} = \hat{x}_n + K \left(\begin{bmatrix} i_{ds} \\ i_{qs} \end{bmatrix} - H x'_n \right) \quad (12)$$

Step 5: correction of the covariance matrix error

$$P = P' \quad (13)$$

2.4. Fuzzy PI controller

The PI fuzzy controllers were commonly studied recently to handle nonlinear systems. The control law is identified based on a principle of knowledge and a fuzzy logic conclusion technique. The knowledge part includes a string of the expression (IF. . THEN) rules with ambiguous files. The fuzzy PI controller is applied to promote the outcomes of the IM system via tuning the PI control gains and then matching the desired response. PI rules are similar to FLC in design and have shown in Table 2.

The proposed fuzzy PI controller has five fuzzy sets with functions united and spread out on each (normalized) world. The input membership functions are a triangular type for the error signal. However, the other five memberships are for the error rate. The output memberships are two: one for and the second in [22], [23]. The input and output memberships have clarified in Figure 3.

Table 2. Rules for determination of K_p and K_i respectively

de/e	NB	NM	Z	PM	PB
NB	G	P	G	P	G
NM	G	G	G	G	G
Z	G	G	G	G	G
PM	G	G	G	G	G
PB	G	P	G	P	G
NB	G	G	G	G	G
NM	P	G	G	G	P
Z	P	P	G	P	P
PM	P	G	G	G	P
PB	G	G	G	G	G

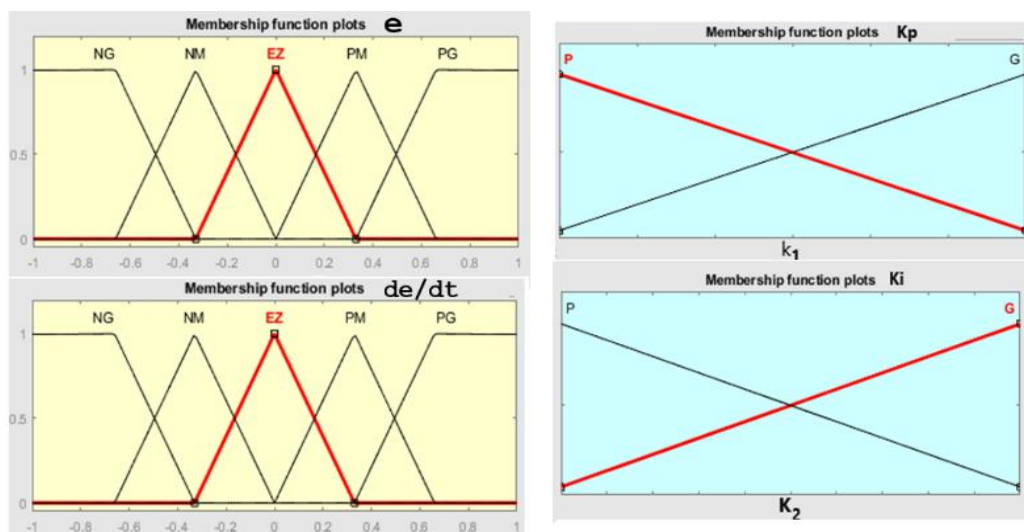


Figure 3. Input and output memberships

2.5. Grey wolf optimizer

Grey wolves (GWs) live in a group and chase prey with a plan. GWs are categorized into four classes. The wolf leaders, called alphas, are mainly in charge of making decisions and yet permit mating in the bundle. The betas have enhanced the alpha in making decisions. The beta wolf is the superior nominate to become the alpha. The beta wolf must consider the alpha besides commanding the rest of the lower-level wolves. The omega is considered the minimum ranking of GWs and occupies the position of the scapegoat. Omegas always have to give in to all the other controlling wolves. Nevertheless, delta wolves are subject to alphas and betas, and both govern the omega. The candidate solutions of GWO are alpha, beta, and delta, respectively. GWs encircle victims during the chase, as illustrated in Figure 4. The wolf position vector is updated according to the prey position vector \bar{X}_p by [24], [25]:

$$\bar{X}(t+1) = \bar{X}_p(t) - \bar{A} \cdot |\bar{C} \cdot \bar{X}_p(t) - \bar{X}(t)| \quad (14)$$

where, the present iteration is t , \bar{A} and \bar{C} are the vectors of the coefficient computed underneath.

$$\bar{A} = 2\bar{a} \cdot \bar{r}_1 - \bar{a}$$

$$\bar{C} = 2 \cdot \bar{r}_2$$

$$\bar{a} = 2 - 2 \frac{t}{\text{Maximum Iterations}} \text{ reduced from 2 to 0, where } r_1 \text{ and } r_2 \text{ are incidental vectors in } [0,1]$$

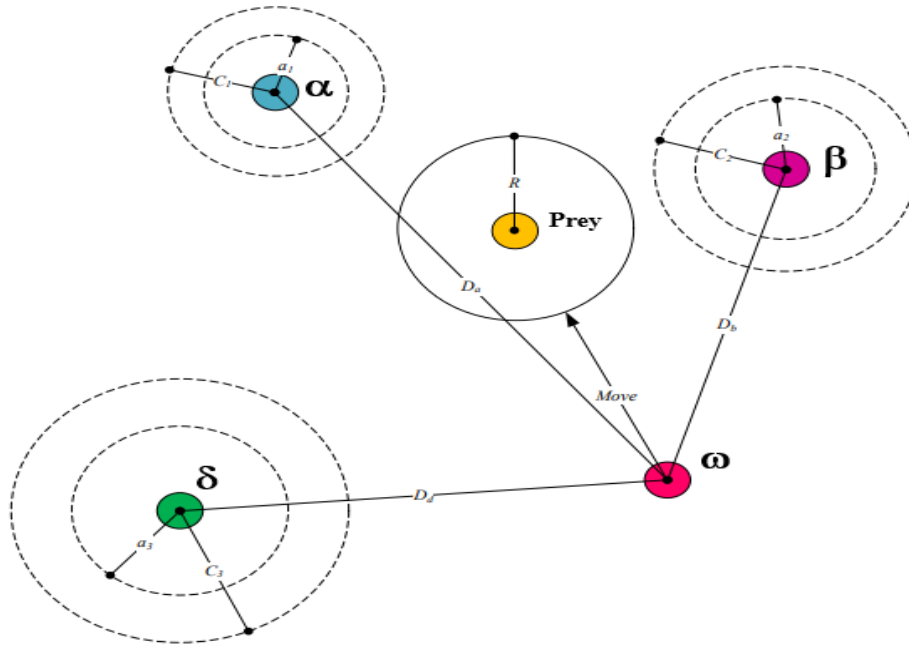


Figure 4. Position update in GWO

The GWs can acknowledge the place of victims and then surround them. Ordinarily, the alpha is in charge of guiding the chasing process. Furthermore, beta and delta as well as participated in chasing on occasion. Nonetheless, in a search space, the optimum position of the (prey) isn't predefined. Assume that the alpha considered a better prospect solution, while the delta and beta wolves have supreme wisdom regarding the position of the potential prey. Thus, keep the initial three most profitable outcomes gained yet and enforce the rest mechanisms comprising the omegas to revamp their places due to the location of the most acceptable agent. The suggested formulas are in the following consideration.

$$\bar{D}_\alpha = |\bar{C}_1 \bar{X}_\alpha - \bar{X}|, \bar{D}_\beta = |\bar{C}_2 \bar{X}_\beta - \bar{X}|,$$

$$\bar{D}_\delta = |\bar{C}_3 \bar{X}_\delta - \bar{X}| \quad (15)$$

$$\bar{X}_1 = \bar{X}_\alpha - \bar{A}_1 \cdot (\bar{D}_\alpha), \bar{X}_2 = \bar{X}_\beta - \bar{A}_2 \cdot (\bar{D}_\beta),$$

$$\bar{X}_3 = \bar{X}_\delta - \bar{A}_3 \cdot (\bar{D}_\delta) \quad (16)$$

$$\bar{X}(t+1) = \frac{1}{3}(\bar{X}_1 + \bar{X}_2 + \bar{X}_3) \quad (17)$$

The GWO algorithm steps are [25]:

Step 1: initialization

Initialize population of GWs is X_i ($i = 1, 2, \dots, n$) preface an a, A, and C

Step 2: compute the suitability per tracking agent

\bar{X}_α =the best search agent

\bar{X}_β =the second best search agent

\bar{X}_δ =the third best search agent

Step 3: recalculate the location of the present search agent

Step 4: renew each of a, A, and C

Step 5: compute the comprehensive fitness of whole search agents

Step 6: update the X_α , X_β , and X_δ

Step 7: end the procedure if ($t < \text{Max number of iterations}$)

Step 8: go to Step 3

3. RESULTS AND ANALYSIS

The Simulink model of DTC of three-phase IM has displayed in Figure 5. This model is used to overcome the load variation and ripple minimization by using an intelligent (PI) controller. Utilized motor parameters are proposed in Table 3. The IM is loaded at instant $t=2$ s and unloaded at $t=4$ s. The error signals obtained for the flux value of the stator and the electromagnetic torque with their estimated magnitudes, respectively. Then the error values are submitted to the hysteresis controllers. A proper voltage vector has chosen by relying on the inverter potential Table 1. In the voltage inverter, the pulses (SA), (SB), and (SC) are in charge of controlling the switching power as well as established from the switching table.

The PI controllers supply feedback signals to the system. GWO with (10) search agents and (40) iterations considered the best solutions are (110.869) and (4.189). The minimum fitness has been deemed the value (0.002351). The speed response obtained is clarified in Figure 6. It is clear that the PI controllers overcome the overshoot during startup, overcome the loading effect, and decline the steady-state error. The proper tuning of the EKF gives a better estimation of speed, stator currents, rotor position, and torque which are illustrated in Figures 7-10, respectively. The estimated parameters are with minimum ripple.

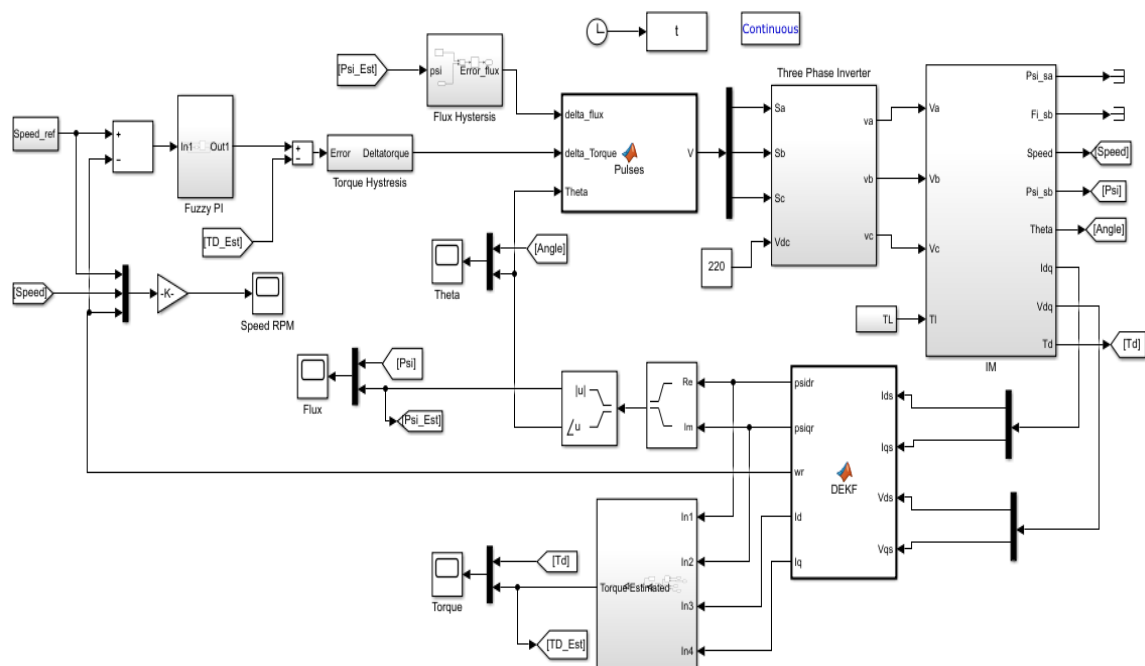


Figure 5. Sensor less DTC of IM simulation

Table 3. Motor parameters

Parameters	Rated value
Voltage	250 V
Frequency	50 Hz
No. of poles	6
Stator resistance	6.75 Ω
Rotor resistance	6.21 Ω
Stator inductance	0.5192 H
Rotor inductance	0.5192 H
Mutual inductance	0.2848 H
Moment of inertia	0.018 kg. m ²
Coefficient of viscous friction	0.003 N. s/rad

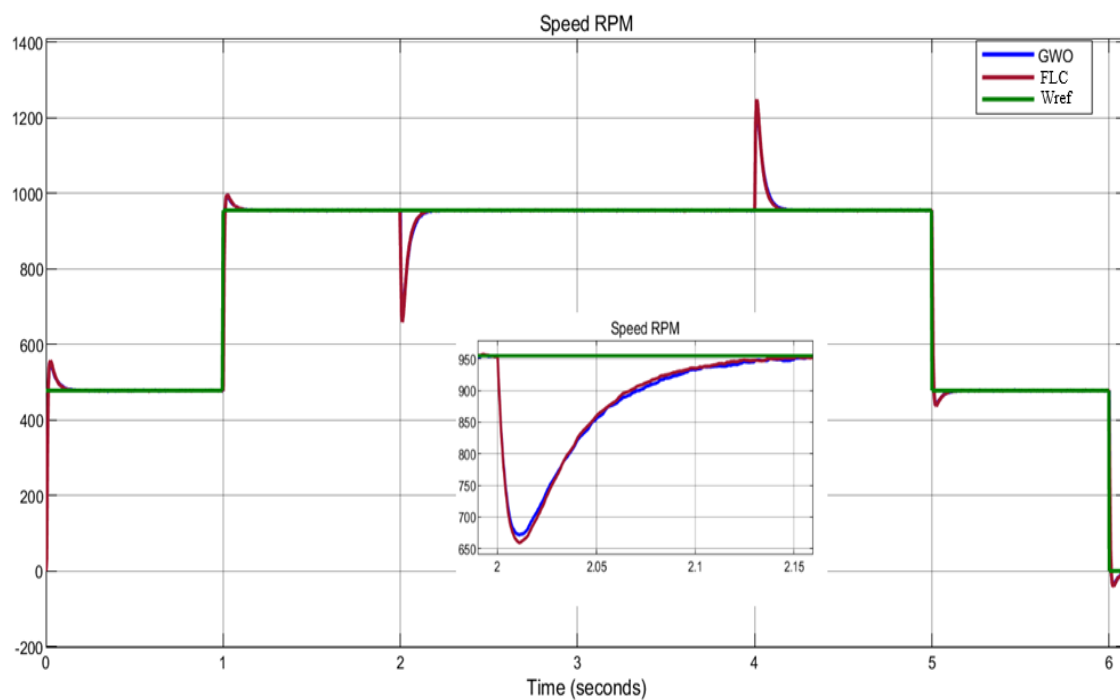


Figure 6. Speed responses due to PI controllers

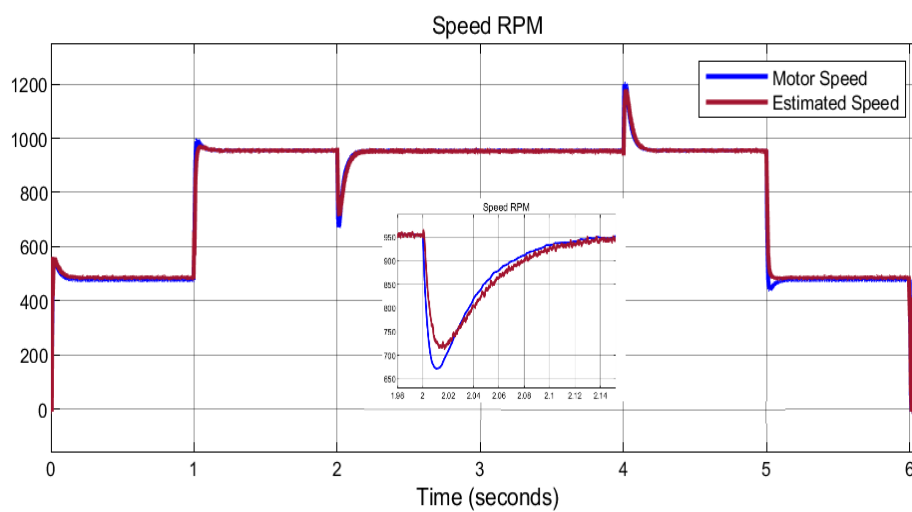


Figure 7. Speed estimated by EKF

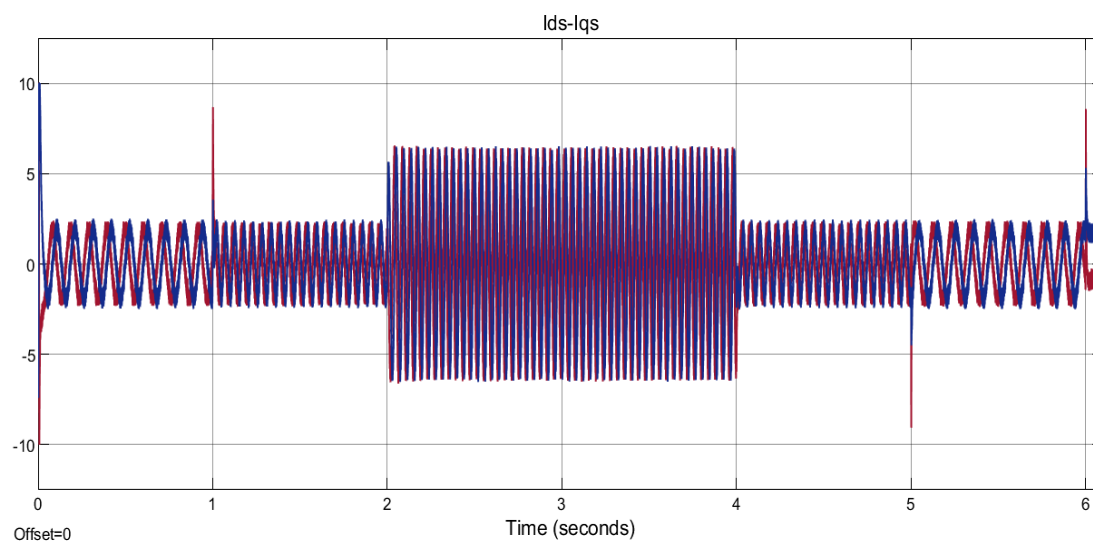
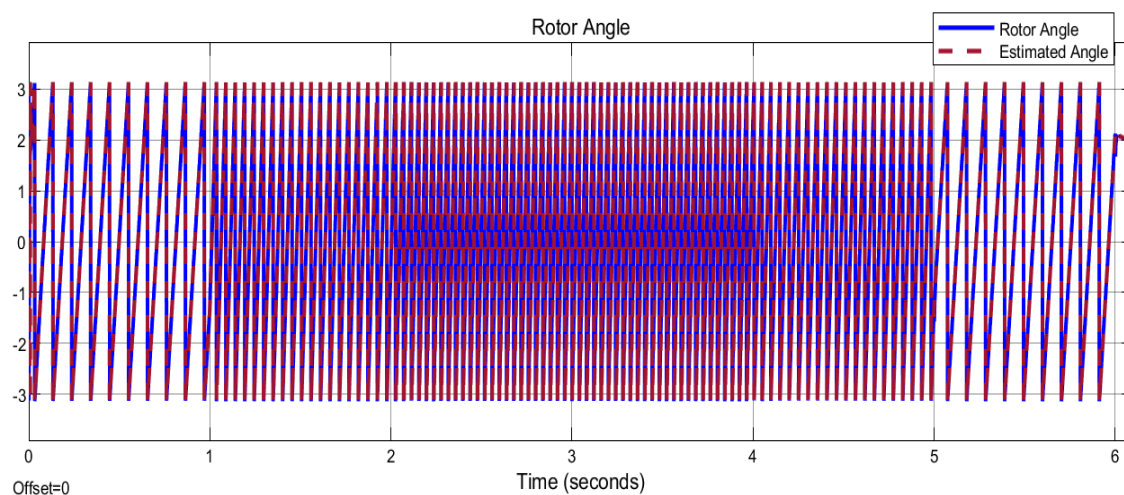
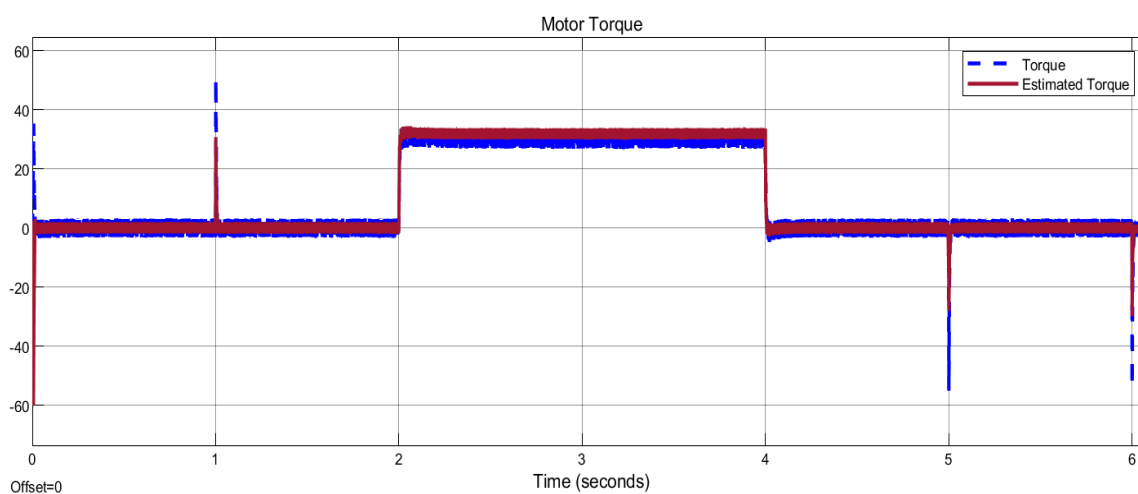
Figure 8. Estimated stator currents \hat{I}_d and \hat{I}_q Figure 9. Estimated rotor angle ($\hat{\theta}$)

Figure 10. Estimated torque

4. CONCLUSION




The fuzzy PI controller proposed to eliminate the ripples in motor states and makes the system overcome the load changes. A satisfy tuning, the system parameters and observation covariance matrices will uncover a better estimation of the required system states. The DEKF is very sensitive to the sampling time, Q matrix, and R matrix. Easy implementation of the GWO is due to a simple structure and smaller storage required. Because of little of the decision variables and the continuous decrease of search space, in GWO the convergence is more rapid. Moreover, two base parameters are only must be taken into consideration to be adjusted.

REFERENCES




- [1] C.-M. Ong, *Dynamic Simulations of Electric Machinery: Using MATLAB SIMULINK* in United States of America: Prentice Hall PTR, vol. 5, 1998.
- [2] A. N. Abdullah and M. H. Ali, "Direct torque control of IM using PID controller," *International Journal of Electrical and Computer Engineering (IJECE)*, vol. 10, no. 1, p. 617, Feb. 2020, doi: 10.11591/ijece.v10i1.pp617-625.
- [3] S. N. Manias, "Introduction to Motor Drive Systems," in *Power Electronics and Motor Drive Systems*, Elsevier, 2017, pp. 843–967, doi: 10.1016/b978-0-12-811798-9.00012-3.
- [4] I. Takahashi and T. Noguchi, "A New Quick-Response and High-Efficiency Control Strategy of an Induction Motor," *IEEE Transactions on Industry Applications*, vol. IA-22, no. 5, pp. 820–827, Sep. 1986, doi: 10.1109/tia.1986.4504799.
- [5] F. R. Yasien and M. S. Ali, "Performance Comparison between Conventional PI and PI-Like Fuzzy Speed Controller for Three Phase Induction Motor," *American Academic Scientific Research Journal for Engineering, Technology, and Sciences*, vol. 42, no. 1, no. 1, Apr. 2018.
- [6] M. N. Abdullah, A. T. Humod, and F. H. Faris, "A Comparative Study of PI and IP Controllers For Field Oriented Control of Three Phase Induction Motor," *Iraqi journal of computers, communications, control and systems engineering*, vol. 19, no. 2, 2019.
- [7] S. W. Shneen, H. S. Dakheel, and Z. B. Abdulla, "Design and implementation of variable and constant load for induction motor," *International Journal of Power Electronics and Drive Systems (IJPEDS)*, vol. 11, no. 2, pp. 762–773, Jun. 2020, doi: 10.11591/ijpeds.v11.i2.pp762-773.
- [8] F. Rafeek and Z. Khudher, "Design of Fuzzy-Like Position Controller for Permanent Magnet Stepper Motor," *Iraqi journal of computers, communication, control and systems engineering*, vol. 16, no. 1, pp. 84–91, Feb. 2016.
- [9] N. E. Ouanjli *et al.*, "Modern improvement techniques of direct torque control for induction motor drives - a review," *Protection and Control of Modern Power Systems*, vol. 4, no. 1, pp. 1–12, May 2019, doi: 10.1186/s41601-019-0125-5.
- [10] V. Kostić, M. Petronijević, N. Mitrović, and B. Banković, "Experimental verification of direct torque control methods for electric drive application," *Facta Universitatis, Series: Automatic Control and Robotics*, vol. 8, no. 1, pp. 111–126, 2009.
- [11] F. R. Yaseen and W. H. Nasser, "Design Of Speed Controller For Three Phase Induction Motor Using Fuzzy Logic Approach," *Iraqi Journal Of Computers, Communications, Control And Systems Engineering*, vol. 18, no. 3, pp. 12–25, Dec. 2018.
- [12] M. Vasudevan, "Improved direct torque control strategy with ripple minimization for induction motor drive," Anna University, Tamil Nadu, India, 2006.
- [13] T. O-Kowalska, M. Korzonek, and G. Tarchala, "Performance Analysis of Speed-Sensorless Induction Motor Drive Using Discrete Current-Error Based MRAS Estimators," *Energies*, vol. 13, no. 10, p. 2595, May 2020, doi: 10.3390/en13102595.
- [14] A. J. Hamidi, A. A. Ogla, and Y. N. Ibrahim, "State Estimation of Two-Phase Permanent Magnet Synchronous Motor," *Engineering and Technology Journal*, vol. 27, no. 7, pp. 1435–1443, May 2009.
- [15] D. Wang, B. Song, C. Kang, and J. Xu, "Design of Fractional Order PI Controller for Permanent Magnet Synchronous Motor," in *2018 2nd IEEE Advanced Information Management, Communication, Electronic and Automation Control Conference (IMCEC)*, May 2018, doi: 10.1109/imcec.2018.8469310.
- [16] Y. Zhang, Z. Yin, J. Liu, and X. Tong, "Design and Implementation of an Adaptive Sliding-Mode Observer for Sensorless Vector Controlled Induction Machine Drives," *Journal of Electrical Engineering and Technology*, vol. 13, no. 3, pp. 1304–1316, 2018, doi: 10.5370/JEET.2018.13.3.1304.
- [17] S. R. Apsha and C. J. N., "A Fuzzy Logic based Sensorless Speed Control of DTC-SVM of an Induction Motor using EKF," *IJIREICE*, vol. 3, no. 11, pp. 115–118, Nov. 2015, doi: 10.17148/ijireeice.2015.31124.
- [18] A. M. Trzynadlowski, "Control of Induction Motors," in *Control of Induction Motors*, San Diego: Academic Press, 2001, pp. 1–228, doi: 10.1016/B978-012701510-1/50001-5.
- [19] T.-F. Chan and K. Shi, *Applied Intelligent Control of Induction Motor Drives*. Wiley-IEEE Press, 2011, doi: 10.1002/9780470825587.
- [20] B. K. Bose, *Modern Power Electronics and AC Drives* in United States of America: Prentice Hall PTR, 2002.
- [21] D. Simon, *Optimal State Estimation: Kalman, H Infinity, and Nonlinear Approaches*, 1st edition. Hoboken, N.J.: Wiley-Interscience, 2006.
- [22] J. Kluska, "Analytical Methods in Fuzzy Modeling and Control," in *Analytical Methods in Fuzzy Modeling and Control*, J. Kluska, Ed. Berlin, Heidelberg: Springer, 2009, pp. 1–216, doi: 10.1007/978-3-540-89927-3_1.
- [23] S. N. Sivanandam, S. Sumathi, and S. N. Deepa, Eds., "Introduction to Fuzzy Logic using MATLAB," in *Introduction to Fuzzy Logic using MATLAB*, Berlin, Heidelberg: Springer, 2007, pp. 1–430, doi: 10.1007/978-3-540-35781-0_1.
- [24] S. Mirjalili, S. M. Mirjalili, and A. Lewis, "Grey Wolf Optimizer," *Advances in Engineering Software*, vol. 69, pp. 46–61, Mar. 2014, doi: 10.1016/j.advengsoft.2013.12.007.
- [25] Y. Li, X. Lin, and J. Liu, "An Improved Gray Wolf Optimization Algorithm to Solve Engineering Problems," *Sustainability*, vol. 13, no. 6, p. 3208, Mar. 2021, doi: 10.3390/su13063208.

BIOGRAPHIES OF AUTHORS






Yaser Nabeel Ibrahim Alothman    has graduated from the Department of Control and Systems Engineering at the University of Technology. He worked as Assistant Lecturer in the same department from 2004 to 2010. He received his scientific promotion to a University Lecturer in 2010. In 2013 he was granted a Ph.D position in the Iraqi-British Scholarship Program. He was accepted to Essex University in Great Britain as a Ph.D student in October 2013 under the supervision of Dr Dong bing Guo until December 2018, when he received his PhD degree. He returned to the Department of Control and Systems Engineering at his home University in Baghdad to work as a Ph.D lecturer. He can be contacted at email: 60005@uotechnology.edu.iq.



Wisam Essmat Abdul-Lateef    current position member of staff of the University of Technology, Department of Electromechanical and received the Engineer degree in Mechanical Engineering from the Department of Mechanical Engineering/University of Technology/Baghdad-Iraq. He received a Master's degree (M.Sc) degree in Mechanical Engineering (Design)–in 2004 from the Department of Mechanical Engineering/University of Technology/Baghdad–Iraq. He received his Ph.D degree in Mechatronics and robotic systems–in 2017 from Platov South-Russian University (NPI)/Department of Mechatronics and Automation/Rostov-on-Don (Russian). He can be contacted at email: 50110@uotechnology.edu.iq.



Sabah Abdul-Hassan Gitaffa    holds a degree of MS.C in Electrical Engineering from the University of Technology, Baghdad-Iraq in 2004. He received his B.Sc (Electrical Engineering) from Al-Rashed College of Engineering and Science, Iraq in 1999. He is currently an assistant professor at the Department of Electrical Engineering at the University of Technology, Baghdad, Iraq since September 2003. His research includes image processing, FPGA, digital signal processing, control sensor system, robotic engineering and smart system, MOSFET miniaturization design, and hiding Secured design. He has published over 20 papers in international journals and conferences. He can be contacted at email: sabah.a.gitaffa@uotechnology.edu.iq.